Middle Pleistocene to Holocene activity of the Gondola Fault Zone (Southern Adriatic Foreland): deformation of a regional shear zone and seismotectonic implications

Domenico Ridente [a], Umberto Fracassi [b], Daniela Di Bucci [c], Fabio Trincardi [a], Gianluca Valensise [b]

[a] Istituto di Scienze Marine (ISMAR – Geologia Marina), CNR. Via Gobetti, 101 - 40129 Bologna, Italy

[b] Istituto Nazionale di Geofisica e Vulcanologia. Via di Vigna Murata, 605 - 00143 Roma, Italy

[c] Dipartimento della Protezione Civile. Via Vitorchiano, 4 - 00189 Roma, Italy

Corresponding author:

Domenico Ridente

Istituto di Scienze Marine (ISMAR – Geologia Marina), CNR

Via Gobetti, 101 - 40129 Bologna, Italy

domenico.ridente@bo.ismar.cnr.it

phone number: +39-051-6398872

Key words: Quaternary; Foreland deformation; Active fault; Adriatic Sea.

Abstract

Recent seismicity in and around the Gargano Promontory, an uplifted portion of the southern Adriatic Foreland domain, indicates active E-W strike-slip faulting in a region that has also been struck by large historical earthquakes, particularly along the Mattinata Fault. Seismic profiles published in the past two decades show that the pattern of tectonic deformation along the E-W–trending segment of the Gondola Fault Zone, the offshore counterpart of the Mattinata Fault, is strikingly similar to that observed onshore during the Eocene-Pliocene interval. Based on the lack of instrumental seismicity in the south Adriatic offshore, however, and on standard seismic reflection data showing an undisturbed Quaternary succession above the Gondola Fault Zone, this fault zone has been interpreted as essentially inactive since the Pliocene. Nevertheless, many investigators emphasised the genetic relationships and physical continuity between the Mattinata Fault, a positively active tectonic feature, and the Gondola Fault Zone. The seismotectonic potential of the system formed by these two faults has never been investigated in detail. Recent investigations of Quaternary sedimentary successions on the Adriatic shelf, by means of very high-resolution seismic-stratigraphic data, have led to the identification of fold growth and fault propagation in Middle-Upper Pleistocene and Holocene units. The inferred pattern of gentle folding and shallow faulting indicates that sediments deposited during the past ca. 450 ka were recurrently deformed along the E-W branch of the Gondola Fault Zone.

We performed a detailed reconstruction and kinematic interpretation of the most recent deformation observed along the Gondola Fault Zone and interpret it in the broader context of the seismotectonic setting of the southern Apennines-foreland region. We hypothesise that the entire 180 km-long Molise-Gondola Shear Zone is presently active and speculate that also its offshore portion, the Gondola Fault Zone, has a seismogenic behaviour.

1. Introduction

Foreland basins are subject to long-term tectonic evolution, display marked structural segmentation and can be dissected by tectonic lineaments of variable extent originating from re-activation of inherited fault systems (Allen et al., 1986). In some cases, foreland deformation can evolve into complex strike-slip fault systems that accommodate large-scale strain partitioning during active subduction and continental collision (Doglioni et al., 1994). Tectonic activity along these structures can bear the effects of the deformation along the thrust belt and thrust front, and may be associated with intense upper crustal seismicity. After the inception of a deformation zone within a foreland sector, reactivation may occur in response to a new stress field different from that active during thrusting. Therefore, foreland basins display deformational styles that may be especially difficult to interpret, being the expression of both the nature of different stress fields and of the original orientation of pre-existing faults and tectonic lineaments. This also implies a difficulty in the determination of the present activity and seismogenic potential of foreland deformation zones.

Until just a few years ago, the active tectonics of the Italian peninsula was believed to be dominated by SW-NE oriented extension occurring along the axis of the Apennines (Montone et al., 2004) and responsible for severe earthquakes generated by large NW-SE normal faults (Galadini et al., 2001; Valensise and Pantosti, 2001; Fig. 1).

The 2002 Molise earthquakes (M=5.8; notice that, if not differently reported, all magnitudes in this paper are from CPTI Catalogue; Gruppo di Lavoro CPTI, 2004; Fig. 1b), however, located to the NE of the Southern Apennine axis, supplied living evidence that in this sector of the chain (i.e. toward the Adriatic Foreland) NW-SE normal faulting gives way to relatively deep E-W, right-lateral seismogenic faults. Further to the east, in the Southern Adriatic Sea, very high-resolution seismic-stratigraphic data indicate that also the marine portion of the Adriatic Foreland is being actively deformed along E-W inherited tectonic structures (Ridente and Trincardi, 2006). This combined evidence suggests that the Southern Adriatic Foreland is affected by active E-W fault systems, both on- and offshore, buried and exposed, possibly organised in regional shear zones (Di Bucci and Mazzoli, 2003; Valensise et al., 2004; both with references).

Major E-W–oriented shear zones have been singled out roughly between the latitudes 40°30'N and 42°30'N (Favali et al; 1993; Doglioni et al., 1994). Among them, the Molise-Gondola Shear Zone (MGSZ) has a clear E-W structural trend and is positively seismogenic in its western-most part (Di Bucci et al., 2006, and references therein; Fig. 1a). This shear zone, whose present activity is interpreted as due to the reactivation of an inherited zone of weakness, includes (from west to east) the source region of the 2002 Molise earthquakes, that of the 1627 Gargano earthquake, the Mattinata Fault on the mainland, and the Gondola Fault Zone offshore (Fig. 1). In spite of the detailed studies concerning each strand of the MGSZ, an integrated analysis of its onshore and offshore parts is still lacking, except for the general perspective provided by the analogue models of the entire shear zone (Di Bucci et al., 2006).

While the existence of E-W–oriented seismogenic faults in the Molise area is a newly acquired notion, the eastward extent and the geodynamic relevance of the offshore counterpart of the Mattinata Fault, i.e. the Gondola Fault Zone, have long been recognized (Finetti, 1984). However, the present activity of the Gondola Fault Zone is poorly constrained if compared with the rest of the MGSZ. Based on high-resolution seismic-stratigraphic data, Ridente and Trincardi (2006) provided the first direct evidence for Late Quaternary deformation.

Although the Mattinata and Gondola faults may appear as two portions of the same system extending onshore and offshore (e.g., Piccardi, 2005), the assumption of a coupled long-term evolution and of a similar behaviour under a given stress field is not straightforward. In spite of their similar E-W strike and alignment, the different sectors of the MGSZ exhibit significant differences in their behaviour. In particular, moving from the offshore to the onshore, evidence for active tectonics along this regional shear zone is supplied by:

- recent deformation (up to Late Holocene) along the Gondola Fault Zone (Ridente and Trincardi, 2006), where, however, significant instrumental seismicity has never been recorded, with the exception of a few moderate events north of the study area (Fig. 1b);
- extensive surface evidence of activity (up to 50-60 km) along the Mattinata Fault (Piccardi, 2005; Tondi et al., 2005) and blind faulting along the Apricena Fault (Patacca and Scandone, 2004a), interpreted as a surficial splay of the MGSZ by Di Bucci et al. (2006; Fig. 1). Both these portions of the MGSZ are associated with the historical seismicity of the Gargano region, where also frequent instrumental seismicity occurs;
- severe seismicity in the Molise region (2002 Molise earthquakes, M=5.8) revealing right-lateral strike-slip faulting on E-W blind faults.

To better constrain the recent deformation along the Gondola Fault Zone, we carried out an in-depth analysis of Middle-Upper Pleistocene and Holocene tectonic deformation along its E-W branch. We used a dense network of very high-resolution Chirp-Sonar seismic profiles (Fig. 2) to map in detail first order gentle fold systems and faults propagating in shallow deposits (locally up to the seafloor) that are Middle-Upper Pleistocene and Holocene in age. Our main result is the detailed reconstruction of the geometry, lateral continuity and activity of a ~50-km-long deformation zone corresponding to the E-W branch of the Gondola Fault Zone. We focus on the kinematic interpretation of this shallow deformation zone and compare our results with the active deformation and seismicity characterising other sectors of the MGSZ. We then (i) discuss the hypothesis that the MGSZ is being actively deformed as a whole and (ii) speculate about the possible seismotectonic implications of this activity.

2. Geological setting

2.1. Regional outline

The Apennine fold-and-thrust belt is part of a Late Cenozoic accretionary wedge (e.g., Patacca and Scandone, 1989). All along the Italian peninsula, this wedge borders a foreland basin, shared with the Alpine and Dinaride Chains, whose southern portion corresponds with the Adriatic Sea and the Apulia region. These are part of "Adria", an independent microplate or a promontory of the African plate, according to one of the most lively controversies in Mediterranean plate tectonics (Channell et al., 1979; Anderson, 1987; Catalano et al., 2001; Wortman et al., 2001). The Southern Apennines are formed by east-to-northeast verging thrust sheets (Fig. 1) deriving from palaeogeographic domains of alternating carbonate platforms and pelagic basins (Mostardini and Merlini, 1986). The outermost of these domains is represented by the Apulia Platform, a ~6 km-thick succession of shallow-water, Mesozoic carbonate rocks (Ricchetti et al., 1988; Ciaranfi et al., 1988). The lowermost ~1,000 m of this succession are made up of Triassic anhydrite-dolomite deposits (Butler et al., 2004), in turn underlain by fluvial-deltaic Permo-Triassic deposits (Bosellini et al., 1993; Butler et al., 2004) and by an igneous/metamorphic Palaeozoic basement (Chiappini et al., 2000; Tiberti et al., 2005). The Apulia Platform and underlying basement are partly involved in the orogenic wedge, partly form the foreland inflected below the outer front of the Apennines, and partly form the exposed foreland of the Apulia Peninsula, the Gargano Promontory and the Southern Adriatic Sea (Fig. 1a). For the sake of simplicity, we will simply refer to the Adriatic Foreland, regardless of the above domains.

During the emplacement of the Apennines Chain (from Oligo-Miocene up to Early Pleistocene), the Adriatic Foreland was laterally partitioned into distinct tectonic domains (e.g., Ricci Lucchi, 1986). Partitioning was driven by a north-south differentiation of the westward-dipping Adriatic lithosphere, affected by significant discontinuities and thickness variations (Calcagnile and Panza, 1981; Royden et al., 1987; Doglioni et al., 1994). Thrusting of the Southern Apennines progressed toward the Adriatic Foreland up to the beginning of the Middle Pleistocene, when motion at the wedge front is reported to have ceased (Patacca and Scandone, 2004b). A geodynamic change must have taken place around 800 ka BP, when SW-NE extension became dominant along the axis of the Apennines (Cinque et al., 1993; Galadini, 1999; D'Agostino et al., 2001). This tensional regime is still active, though in the core of the foreland NW-SE horizontal compression accompanies the SW-NE tension (Vannucci and Gasperini, 2004).

2.2. The onshore portion of the MGSZ

The E-W striking MGSZ has been described as roughly running at the latitude 41°40'N and can be traced for a total length of at least 180 km (Di Bucci et al., 2006). Overall, the system appears as a ~15 km wide corridor from the Adriatic Sea to the core of the Apennines. Its onshore portion includes, from east to west, the Mattinata Fault, the Chieuti High, and the seismogenic faults responsible for the 2002 Molise earthquakes (Fig. 1).

The Mattinata Fault cuts through the Gargano Promontory, an E-W elongated relief (maximum elevation ~1,000 m) along the flexural bulge of the Adriatic Foreland. It corresponds to a poly-phased belt of intense deformation, including several fault splays, and has been intensely investigated from a regional, structural and seismotectonic point of view (Finetti, 1982; Ortolani and Pagliuca, 1987; Funiciello et al., 1988; Winter and Tapponier, 1991; Favali et al., 1993; Piccardi, 1998; 2005; Bertotti et al., 1999; Salvini et al., 1999; Billi and Salvini, 2000; Chilovi et al., 2000; Billi, 2003; Borre et al., 2003; Billi et al., 2007). Most investigators (but not all; see for example Billi et al., 2007) agree on a present-day right-lateral main component of motion, as confirmed by earthquakes focal mechanisms (e.g., 19 June 1975, Mw 5.1; 30 September 1995, Mw 5.2; 29 May and 5 October 2006, Mw 4.6 and 4.2 respectively; these latter from

MEDNET, 2006; Fig. 1b), GPS data (Anzidei et al., 1996; Ferranti and Oldow, 2005), geomorphological and palaeoseismological investigations (Piccardi, 1998; 2005; Borre et al., 2003; Tondi et al., 2005). Moreover, the Mattinata Fault has been interpreted as the source of large historical earthquakes (e.g., 493 A.D., Baratta, 1901, quoted in Piccardi, 1998; 6 December 1875, Mw 6.1; Valensise and Pantosti, 2001; DISS Working Group, 2006), and instrumental seismicity is recorded within the uppermost 25 km of the crust throughout the Gargano Promontory (Chiarabba et al., 2005; Castello et al., 2006).

Further to the west, the foreland plunges below the Pliocene-Pleistocene deposits filling the Bradanic Trough, the most recent foredeep of the Southern Apennines (Mariotti and Doglioni, 2000; Fig. 1). In this sector, an E-W ridge known as the Chieuti High (Casnedi and Moruzzi, 1978; Fig. 1) is preserved at the top of the buried Apulia Platform along strike of the Mattinata Fault. This structure, recently interpreted as an inherited push-up related to Cenozoic strike-slip motion (Patacca and Scandone, 2004a), is accompanied by WNW-ESE–striking, SSW dipping faults with a normal component of motion. Patacca and Scandone (2004a) interpret one of these faults, namely the Apricena Fault (Fig. 1), as the source of the 30 July 1627 Gargano earthquake (M 6.7; Fig. 1b).

West of the Chieuti High, where the Adriatic Foreland deepens to the west below the outer front of the Apennines, lies the source region of the 31 October and 1 November 2002 Molise earthquakes (Fig. 1). The two mainshocks of the Molise earthquake sequence had similar magnitude (Mw 5.8-5.7) and hypocentral depth (16-18 km; Vallée and Di Luccio, 2005), and both exhibit a pure strike-slip focal mechanism with right-lateral motion on E-W planes (Fig. 1b). Permanent surface deformation revealed by GPS is consistent with this kinematics (Giuliani et al., 2007) and the aftershock distribution also follows an E-W trend, yet no surface faulting was seen following these earthquakes. Overall, the 2002 earthquakes show that E-W striking faults belonging to the MGSZ are solicited under the present-day stress field.

Large discrepancies are found in the literature concerning the amount of displacement along the MGSZ. For instance, Chilovi et al. (2000) suggest that the right-lateral displacement related to the most recent activity of the Mattinata Fault started in Late Pliocene. On this basis, they ascribe to the interval Late Pliocene-Present a horizontal displacement of 15 km, implying a slip-rate of about 6 mm/a. However, this 15 km estimate was proposed by De' Dominicis and Mazzoldi (1987) as a cumulative value for the entire slip history of the Gondola Fault Zone. In contrast, based on offset streams and on more subtle landscape features, Piccardi (1998) proposes a horizontal component of the slip-rate in the order of 1 mm/a. Finally, analogue modelling of the MGSZ by Di Bucci et al. (2006) favours the hypothesis that the most recent and present-day activity of the MGSZ has accumulated a right-lateral displacement yielding a slip-rate close to 1.3 mm/a, thus comparable with the figure proposed by Piccardi (1998).

2.3 The offshore portion of the MGSZ: the Gondola Fault Zone

The Gondola Fault Zone has been related to Cenozoic reactivation of pre-existing faults (e.g., Morelli 2002, and references therein). It is neither in direct continuity, nor perfectly aligned, with the Mattinata Fault, showing an underlap of ~20 km and right-stepping of ~5 km (Fig. 3). The Gondola Fault Zone includes several E-W and NW-SE fault segments dissecting the southern Adriatic continental shelf and slope (Fig. 3). These faults define an elongated structural high called "Gondola ridge" (Colantoni et al., 1990; de Alteriis and Aiello, 1993). This buried structural high along the Gondola Fault Zone does not affect the seafloor topography along most of the its E-W portion, which extends ~70 km across the shelf (Ridente and Trincardi, 2002a; 2006). Conversely, a tectonic-related relief visibly affects the seafloor morphology down–slope (see bathymetry in Fig. 2), along the ~50 km-long NW-SE branch of the Gondola Fault Zone (de Alteriis, 1995; Tramontana et al., 1995).

Several investigators discussed on whether the Gondola Fault Zone is still active and playing a role in the complex geodynamic evolution of the Adriatic Foreland (see Ridente and Trincardi, 2006, with references, for a review). Multi-channel seismic data highlight a regular Pliocene-Quaternary succession draping and sealing the faults and structural highs along the E-W branch of the Gondola Fault Zone. This circumstance should imply that deformation along the Gondola Fault Zone must have been active until the Late Pliocene or Early Pleistocene only (Colantoni et al., 1990; Argnani et al., 1993; de Alteriis and Aiello, 1993; Tramontana et al., 1995). Faulted deposits below the base of the Pliocene-Quaternary show a vertical offset of 500-600 m and a downthrown northern side that accommodates a sedimentary succession thicker than that on the southern side (Fig. 3; De' Dominicis and Mazzoldi, 1987). Moving toward the eastern tip of the E-W branch of the fault, the sedimentary cover north and south of the fault zone gradually attains the same thickness and, finally, becomes thicker in the southern block, due to a dip-slip displacement of ~200 m of this side. This variability of the vertical component of displacement is interpreted as evidence for an overall transcurrent kinematics of the Gondola Fault Zone (Colantoni et al., 1990).

Although multi-channel seismic profiles show the Gondola Fault Zone as draped and sealed by the Pliocene-Quaternary cover, Ridente and Trincardi (2006) have recently shown that these low-frequency data lack the resolution needed to determine whether mild recent deformation propagated through shallower deposits, even where the Pliocene-Quaternary cover displays flat-draping reflectors. When imaged by high-resolution seismic profiles, Middle-Upper Pleistocene sequences appear indeed deformed by gentle folds and high-angle faults along the E-W branch of the Gondola Fault Zone (Fig. 4). These folds consist of two gentle anticlines and an interposed syncline; where present, north-dipping subvertical faults show vertical displacement. Locally, the displacement of Holocene deposits can be recognized up to the maximum flooding surface (Fig. 4), a reference layer that marks the flooding and starvation of the seafloor when sea-level attained its modern highstand position, ~5.5 ^{14}C calibrated ka BP (Trincardi et al., 1996; Correggiari et al., 2001; Cattaneo et al., 2003). In some cases, faults even offset the seafloor.

Historical and instrumental seismicity do not provide direct constraints for the activity of the Gondola Fault Zone, possibly owing to difficulties in retrieving information from offshore earthquake sources. With only a few exceptions, the CPTI catalogue locates all earthquakes onshore through an automatic procedure. Nevertheless, some events that are reported on the eastern coast of Gargano may have occurred offshore. For instance, the 10 August 1893 earthquake (Mw 5.4) severely damaged the port of Mattinatella (at the eastern end of the Mattinata Fault) and induced tangible effects on the environment, including offshore gas seepage and surface ruptures, described by contemporary witnesses (Baratta, 1894, reported in Boschi et al., 2000). Given the intensity distribution of this earthquake (Stucchi et al., 2007), its epicentre could well lie offshore the Gargano Promontory.

3. High-resolution seismic and stratigraphic data

The geophysical data used in this study consist of more than 10,000 km of Chirp-Sonar seismic profiles collected by ISMAR-CNR (Bologna) since 1997 (Fig. 2). Chirp-Sonar profiles were shot from 16 hull-mounted transducers, using a 2-7 kHz sweep-modulated bandwidth (equivalent to a 3.5 kHz profiler) that allows vertical resolution in the order of 50 cm and penetration up to 80-100 m. A 2 kJ Sparker, with vertical resolution in the order of few metres and penetration up to 150 m, was also used to investigate a broader depth interval. Track-line positioning was based on D-GPS navigation, assuring a position accuracy of ~10 m, and transformed to geographic coordinates referred to the WGS84 datum. High-resolution seismic profiles allowed us to investigate the uppermost 100 m of the Late Quaternary succession in the Adriatic Sea.

Seismic data were integrated with sedimentological and chronostratigraphic data from sediment cores (Trincardi et al., 1996; Asioli, 1996; Asioli et al., 1999; 2001; Ridente and Trincardi, 2005). In addition, a 71 m-long borehole in the Central Adriatic Sea (drilled within the frame of "PROMESS 1" European Project) allowed the continuous recovery of Late Quaternary deposits. These deposits were dated using tephra layers, isotope curves, pollen spectra, ^{14}C analyses, and foraminifera abundance (Asioli et al., 2005). Based on these chronostratigraphic data, the investigated interval spans the past ~450 ka (Middle-Upper Pleistocene and Holocene). This stratigraphic interval is made up of depositional sequences numbered progressively down-section. On the shelf, these sequences are defined by erosional surfaces labelled ES1 to ES5, from top to bottom. The nature of these sequences and of their bounding surfaces reflects repeated sea level oscillations during alternating glacial-interglacial periods (Trincardi and Correggiari, 2000; Ridente and Trincardi, 2002a, b).

Deposits above the last glacial erosional surface ES1 record the latest Pleistocene and Holocene post-glacial sea level rise. Deposits below ES1 consist of four sequences that record deposition between subsequent Marine Isotope Stages (MIS) as in the following scheme:

- Sequence 1 = MIS 2-6 (20 to 130-150 ka BP);
- Sequence 2 = MIS 6-8 (130-150 to 230-250 ka BP);
- Sequence 3 = MIS 8-10 (230-250 to 330-350 ka BP);
- Sequence 4 = MIS 10-12 (330-350 to 430-450 ka BP).

Individual sequences are up to a few tens of metres-thick, and are mainly composed by "forced-regression" units recording prolonged phases of sea level fall (Ridente and Trincardi, 2002a, b). The impact of tectonic activity on shallow-shelf deposition can be determined based on the nature of forced-regression deposits, typically consisting of shallow water progradational units (Ridente and Trincardi, 2005). Because preservation of forced-regression deposits is strongly limited when there is little accommodation space available (Helland-Hansen and Martinsen, 1996), the thickness and internal architecture of such deposits are highly sensitive to syn-depositional deformation that can modify the accommodation space on the shelf. Superimposed on the eustatic sea level fall, changes in accommodation space induced by tectonic deformation impart variations in the thickness and internal geometry of each sequence (Ridente and Trincardi, 2002b). This tectonic control on the lateral variability of sequences results in a pre- and syn-tectonic depositional pattern at a very local scale. In turn, this pattern allows recognizing where inherited tectonic lineaments have been active recently (Ridente and Trincardi, 2006).

The four Middle-Upper Pleistocene sequences show dominant muddy composition, with thin beds of silt and fine sand occasionally occurring close to the erosion surfaces. Therefore, we considered the possible effect of differential compaction of the underlying Pliocene-Quaternary clastic sediments, that are thinner along the Gondola Fault Zone with respect to the surroundings (Colantoni et al., 1990). Preliminary results indicate differential values of compaction well below 10 m and far from the maximum displacement values measured for some of the faults described in Section 4. Therefore, we conclude that differential compaction is not sufficient to justify the development of the entire deformation belt along the Gondola Fault Zone, and that we are dealing with an active fault system.

4. Active deformation along the E-W branch of the Gondola Fault Zone

4.1. Distribution and lateral variability of the observed deformation

In the study area, the deformation belt along the Gondola Fault Zone encompasses two major similar, asymmetric, gentle, north-verging anticlines. They are both characterised by E-W crest lines and by a ~7 km wavelength (Figs. 4 and 5). The asymmetry of the two folds becomes more evident from east to west, particularly along the northern fold. In figure 5, the anticlines are represented by the crest lines and the flex lines along the limbs, which may be affected by minor undulations (Fig. 6A, C). The northern anticline is over 50 km-long and has an amplitude of ~15 m (measured between the crest and the flexes), locally exceeding 20 m. The southern anticline is ~30 km-long and parallel to the eastern sector of the other anticline. Both folds show an interlimb angle very close to 180°, the maximum real dip of the limbs being ~1° (in particular for the northern ones). The northern limbs of both anticlines are slightly steeper and generally affected by faults that may also be seen along the axis of the northern anticline (Fig. 6C). The expression of these subvertical faults on seismic profiles varies from an abrupt offset of reflectors along distinct fault planes, to shearing of reflectors within tens of metres wide shear zones (Figs. 4 and 6). Fault planes are laterally discontinuous and in some cases are replaced or accompanied by tight folding (Fig. 7) and fluid-escape features (Figs. 4 and 6B), also observed elsewhere in the area (Fig. 5).

The fault system that affects the northern anticline is very well developed; it frequently affects the seafloor and is formed by three branches (Fig. 5). The western branch is more than 8 km-long, has a main subvertical fault plane steeply dipping to the north and exhibits a vertical component of motion (Figs. 5 and 6A). Along this branch, the main slip surface is often accompanied by minor synthetic and antithetic faults. At its western tip, that corresponds to the westernmost tip of the entire system, the ~E-W fault seems to turn into minor N320°-striking faults. Fluid-escape features to the NNW of these minor structures seem to confirm a NW-SE general trend at the western termination of the entire system. Instead, no evidence of deformation is seen to the west of the western branch and related anticline. At the eastern tip of the western branch, the faults transfer the deformation to a set of minor undulations within the main anticline; these minor folds end in correspondence with the principal fault plane of the central branch, thus forming an overstep characterised by soft linkage, at least at the surface.

The central branch is ~18 km-long (Fig. 5) and is characterised by a major subvertical plane, steeply dipping to the north, with a vertical component of motion. Along part of this branch, the main fold is box-shaped with the main fault bounding its northern limb. In its western portion, the central branch is formed by a single fault (Fig. 6B), whereas in its eastern portion it transfers the displacement to another fault through an overstep area of hard linkage. Several minor synthetic and antithetic faults are associated with this second fault (Figs. 4 and 5). At the eastern tip of the central branch, all these faults transfer the deformation to a set of minor undulations and no additional detectable brittle structures occur within the limbs of the main anticline.

Brittle deformation is seen again in the eastern branch (Figs. 5 and 6C), where the main fault is over 5 km-long and only occasionally accompanied by minor faults. With respect to the main fold, and differently from the rest of the structure, the eastern branch of the fault system cuts obliquely the northern anticline and eventually crosses its crest, thus suggesting that it is no longer related to the northern limb of the fold. The eastern tip of this branch is marked by the presence of few minor undulations. Deformation continues east of the area analysed in detail, where a reversal of the downthrown limb is observed (Figs. 5 and 8) and where the Gondola Fault Zone turns from E-W to NW-SE.

Considering the entire northern fold, we notice that the flex line of the northern limb disappears in correspondence with the central branch of the fault system (Fig. 5 and 6B), being involved in the shear zone of the main fault. This is not seen in the southern fold, where faulting along the northern limb is only incipient (Fig. 4) and the continuity of the flex line is preserved.

The overall geometry of the Gondola Fault Zone suggests a significant right-lateral component of motion. The mapped deformation pattern compares to many similar cases described in the literature (see, for instance, the description of the San Andreas Fault south of Brush Mountain in Christie-Blick and Biddle, 1985). This set of features, formed by Riedel shears with minor vertical separation, connected through unfaulted sections where the anticline is best developed, support dextral slip. It is worth noting that the two main north-verging anticlines are not produced by normal-fault dragging. In some cases (Fig. 6C, southern anticline), the anticlines are not even associated with faulting, at least in the studied upper part of the sedimentary sequence. Indeed, the overall deformation pattern described can be explained by a NW-SE striking maximum horizontal stress.

At a more local scale, near-fault hanging-wall deformation, consisting of a small undulation, accompanies the vertical displacement (Fig. 7). This too suggests that the observed faults may well slip with an unresolved lateral component of motion, also considering that 2D seismic sections rarely allow the horizontal component of displacement to be properly detected.

4.2. Age of deformation

As discussed in Section 3, the sequences involved in folding and faulting are precisely dated and this allows us to constrain in detail the Middle-Late Pleistocene and Holocene evolution of the analysed structures. The described pattern of gentle folding and shallow faulting indicates that sediments deposited during the past ~450 ka were repeatedly deformed. This interpretation is supported by syn-tectonic pinch-outs and erosional unconformities occurring at different stratigraphic levels, particularly during the deposition of sequence 2

(~130-230 ka). Younger phases of tectonic growth during deposition of sequence 1 are less easily preserved, probably because the increasing tectonic relief promoted enhanced wave-base erosion in this outer shelf environment.

With respect to the age of brittle deformation, faults can be subdivided into two groups; the first includes faults truncated by the Last Glacial Maximum erosional unconformity (ES1 erosion surface, ~20 ka), while the second includes faults that also offset the overlying uppermost Pleistocene and Holocene deposits and locally the seafloor. Faults belonging to this second group can be found in all three branches, thus supplying direct evidence for present-day activity of the entire structure.

We also investigated syn-tectonic features within stratigraphic units older than those imaged on Chirp data by means of Sparker profiles recently acquired on the Gondola Fault Zone immediately to the east of the study area (Fig. 5), and still under processing. For example, the interpretation of the line drawing of Sparker Profile SE-64 (Fig. 8) allows the following observations:

- anticlinal deformation affects depositional units older than sequence 4 (i.e., below ES5) and clearly impacts the setting of the continental slope;
- syn-tectonic units (i.e., growth strata) commonly observed within sequence 2 to the west are clearly seen in this area also at the base of sequence 3 and below sequence 4, thus indicating fold growth at variable rates during the Middle-Late Pleistocene;
- tectonically-driven unconformities within sequence 2 (between ES2 and ES3), that occur on the facing limbs of the two anticlines, correlate with several episodes of channel incision and filling on the seaward-sloping limb of the northern fold. This observation suggests that the recent tectonic growth may have enhanced outer shelf incision (this interplay has been recognised also further south along the margin, where it has evolved into the inception of the Bari Canyon; Ridente et al., 2007; Fig. 2);
- sequence 3 and older units appear displaced by a fault coincident with the fold axis. Such fault is masked by fluid-escape features in its central part and affects the reflectors with an upward decreasing offset. In this area the southern limb is downthrown, in contrast with the rest of the Gondola Fault Zone, where the northern limb is downthrown.

Finally, with regard to the vertical offset of reflectors all along the investigated fault zone, we remark that the amount of displacement observed varies in space and time (e.g., Fig. 6B); for the Late Pleistocene, it ranges from a few to over 20 m. The highest values are observed along the central branch of the fault system. Where faults affect uppermost Pleistocene and Holocene deposits, displacement values are in the order of 1 m and affect the ES1 surface (~20 ka BP), the maximum flooding surface (~5.5 ka BP) and the seafloor. The vertical component of the slip-rate estimated for displaced Middle-Upper Pleistocene deposits (with reference to ES3 and ES2) ranges between ~0.01 and ~0.16 mm/a. The vertical component of the slip-rate estimated for the uppermost Pleistocene-Holocene is a more constant ~0.05 mm/a, therefore within the range inferred for the Middle-Late Pleistocene.

5. Discussion and conclusions

We reconstructed in detail the geometry and activity of a ~50-km-long fault system affecting the offshore portion of the Adriatic foreland. This analysis does not include the NW-SE branch of the Gondola Fault Zone on the continental slope which is the object of ongoing studies. Nevertheless, our new results combined with literature data for the Mattinata Fault allow us to address the following outstanding questions.

- *Kinematics of the Gondola Fault Zone*. Based on the analysis of the deformation pattern of the Gondola Fault Zone, we propose right-lateral slip resulting from NW-SE maximum horizontal stress as the dominant sense of motion along the entire fault system. This hypothesis is supported by a) the general geometry of the Gondola Fault Zone; b) the asymmetry of the associated anticlines, compatible with a compressional component roughly from the south; and c) the reversal of the vertical displacement along the structure from north to south side up (Fig. 5), that is an indication of strike-slip activity (e.g., Christie-Blick and Biddle, 1985) as already pointed out by Colantoni et al. (1990) for older deposits. A further indication on the sense of shearing can be inferred from the geometry of the westernmost tip of the structure, where a N320° fault segment has a normal component of motion that downthrows the hanging-wall towards the NE, consistent with a right-lateral kinematics. Unfortunately, our data do not allow the amount of horizontal displacement to be directly assessed. We can only speculate that the strike-slip kinematics implies a ratio between horizontal and vertical displacement (much) larger than 1.

- *Activity along the entire E-W branch of the Gondola Fault Zone*. The two main folds affecting Upper

Quaternary deposits show comparable shape, wavelength, amplitude and exhibit faulted northern limbs; this combined evidence leads us to ascribe both features to the same deformation system. The identified structure shows a pronounced E-W elongation and geographically coincides with the E-W branch of the Gondola Fault Zone as known from the literature. It is likely that the observed deformation pattern is due to the reactivation of this major inherited lineament. Unfortunately, the available data do not allow us to assess if the E-W branch of the Gondola Fault moves as a whole or if instead deformation is partitioned onto two or three active segments reflecting the branching we identified during this work (Fig. 5).

- *Structural relationships with the Mattinata Fault*. The points discussed above reveal a similarity between the Gondola and the Mattinata Faults that goes far beyond the fact that they both trend E-W. They are both tens of kilometres-long, inherited, active fault systems, characterised at the surface by transcurrent kinematics with a present-day right-lateral component of motion. However, as shown in Subsection 2.3 and confirmed by our data, the Mattinata Fault and Gondola Fault Zone are neither directly connected nor perfectly aligned. The structural relationships between these fault systems hence remain an open question. Based on what we observed at the westernmost tip of the active Gondola Fault Zone, we can hypothesise the presence of a transfer zone between this one and the Mattinata Fault, characterised by second order, NW-SE striking, mainly normal faults (i.e. a strike-slip relay ramp). However, both fault systems are inherited structures; as such, their present-day relationships may be more complex, e.g. controlled by an inherited transfer zone developed under previous tectonic regimes.

- *Comparison of slip-rates along the Mattinata Fault and Gondola Fault Zone*. A comparison of slip rates is possible only for the vertical component of fault dislocation. The ~0.01-0.16 mm/a values estimated in this paper for the main fault along the Gondola Fault Zone are quite smaller than those suggested by Piccardi (2005) for the Mattinata Fault (0.2-0.7 mm/a) based on geomorphic and palaeoseismological analyses, although Piccardi himself considers the upper bound as "surely overestimated". The very nature of the available data, however, and the different methodologies used in the two areas imply differences in the density of data and in the accuracy of chronological constraints that make such comparison not straightforward.

- *Seismotectonic implications*. The Mattinata Fault has already been proposed as the source of severe historical earthquakes (493 A.D. and 1875), and frequent instrumental seismicity is recorded along and around it within the uppermost 25 km of the crust. Based on the similarities between the Gondola Fault Zone and the Mattinata Fault, one could expect that they also share a similar seismicity pattern.

The empirical relationships by Wells and Coppersmith (1994) suggest that the entire E-W branch of the Gondola Fault Zone (~50 km) could generate earthquakes up to magnitude 6.9. Conversely, if we consider the Gondola Fault Zone as broken up into two or three segments, individual earthquake magnitudes could be in the order of 6.0-6.5. The latter scenario is compatible with the magnitude of the 1875 earthquake and with the 10-20 km length of the individual segments proposed for the Mattinata Fault (DISS Working Group, 2006, and references therein). However, neither have significant historical earthquakes been associated with the Gondola Fault Zone, nor has instrumental seismicity been recorded around it. Such difference with the Mattinata Fault could be only apparent, due to the difficulty of detecting and locating seismicity offshore. In the Gargano as much as in many other parts of the world, the location offshore of the historical earthquakes is particularly uncertain. For instance, in Venezuela, a region which has large seismically active areas offshore, Rodriguez and Audemard (2003) pointed out that when the available information is very limited, different interpretation models may lead to markedly contrasting locations for the same earthquake. Moreover, the short time span covered by instrumental records and the unfavourable architecture of seismological networks may conspire in making the seismotectonic characterisation of active areas offshore much more difficult.

In summary, if we (i) consider significant the lack of historical seismicity in the offshore portion of the MGSZ, (ii) take into account that in a transcurrent regime the lack of constraints on the horizontal component of the slip-rates precludes any rigorous reasoning on the degree of activity of the fault systems, and (iii) admit for the sake of discussion that the vertical slip-rate values available for the Gondola Fault Zone and the Mattinata Fault are comparable, we can point at two opposite seismotectonic scenarios:

1) the similarity between the Mattinata Fault and the Gondola Fault Zone is misleading and we are dealing with two truly independent and dissimilar tectonic structures, the first being more active and seismogenic, the second being characterised by moderate activity and by aseismic slip;

2) also the Gondola Fault Zone is a seismogenic fault, though with very low slip-rates, which would explain the lack of seismicity associated with it. Considering the total extent of the fault system, even though possibly fragmented in 10-15 km-long segments, the impact on the seismic hazard of the coastal region would be significant, and therefore this possibility deserves further investigation.

In general, our results on the Gondola Fault Zone support the identification of the MGSZ as a major fault zone producing active shearing along its entire E-W extent, although with variable rates. Our study identifies novel targets for the exploitation of high-resolution stratigraphic reconstructions, which can now be used for (i) identifying active tectonic features and (ii) tackling open seismotectonic issues in marine settings.

Acknowledgments

We are grateful to F. A. Audemard and an anonymous referee for greatly improving the manuscript with their comments and suggestions. We would like to thank also the Editor R. Caputo for reviewing the manuscript and providing many insightful advices. We acknowledge S. Corrado for the useful discussion on decompaction issues. The captain and the crew of CNR R/V Urania are also acknowledged for their support during the campaigns in the study area. Federica Foglini kindly contributed to organizing the geophysical data in a GIS. This study was supported by ISMAR-CNR (European Project EUROSTRATAFORM - EVK3-CT-2002-00079 - and the Italian Project GNDT "Rischi Sottomarini") and by DPC-INGV Project S2, Research Unit 2.4. This is ISMAR-CNR (Bologna) contribution n. 1570.

Cited references

Allen, P.A., Homewood, P., Williams, G.D., 1986. Foreland basins: an introduction. In: Foreland Basins (Allen, P.A., Homewood, P., eds.). Int. Ass. Sed. Special Publication 8, 3-12.

Anderson, H., 1987. Is the Adriatic an African promontory? Geology 15, 212-215.

Anzidei, M., Baldi, P., Casula, G., Crespi, M., Riguzzi, F., 1996. Repeated GPS survey across the Ionian Sea: evidence of crustal deformations. Geophys. J. Int. 127, 257-267.

Argnani, A., Favali, P., Frugoni, F., Gasperini, M., Ligi, M., Marani, M., Mattietti, G., Mele, G., 1993. Foreland deformational pattern in the Southern Adriatic Sea. Annali di Geofisica 36 (2), 229-247.

Asioli, A., 1996. High-resolution foraminifera biostratigraphy in the central Adriatic basin during the last deglaciation: a contribution to the Paliclas Project. In: Palaeoenvironmental analysis of Italian crater lake and Adriatic sediments (Guilizzoni, P., Oldfield, F.L., eds.). Mem. Istit. It. Idrob. 55, 197-217.

Asioli, A., Piva, A., Cattaneo, A., Ridente, D., Trincardi, F., 2005. Preliminary stratigraphy of the hole PRAD1-2 (EC-PROMESS 1 Project, Central Adriatic) on the basis of micropaleontological and geophysical data. EGU General Assembly, Abstract Vol. 7.

Asioli, A., Trincardi, F., Lowe, J.J., Ariztegui, D., Langone, L., Oldfield, F., 2001. Sub-millennial climatic oscillations in the Central Adriatic during the last deglaciation: paleoceanographic implications. Quat. Sc. Rev. 20, 33-53.

Asioli, A., Trincardi, F., Lowe, J.J., Oldfield, F., 1999. Short-term climate changes during the Last Glacial-Holocene transition: comparison between Mediterranean records and the GRIP event stratigraphy. J. Quat. Sc. 14, 373-381.

Baratta, M., 1894. Intorno ai fenomeni sismici avvenuti nella penisola Garganica durante il 1893. Annali dell'Ufficio Centrale Meteorologico e Geodinamico Italiano, s. II, 15 (1), 265-312.

Baratta, M., 1901. I terremoti d'Italia. Torino (Reprinted by Forni Ed., Bologna 1979, 950 pp.).

Bertotti, G., Casolari, E., Picotti, V., 1999. The Gargano Promontory, a contractional belt in the Adriatic plate. Terranova, 11, 168-173.

Billi, A., 2003. Solution slip and separations on strike-slip fault zones: theory and application to the Mattinata Fault, Italy. J. Struct. Geol. 25, 703-715.

Billi, A., Salvini, F., 2000. Sistemi di fratture associati a faglie in rocce carbonatiche: nuovi dati sull'evoluzione tettonica del Promontorio del Gargano. Boll. Soc. Geol. It. 119, 237-250.

Billi, A., Gambini, R., Nicolai, C., Storti, F., 2007. Neogene-Quaternary intraforeland transpression along a Mesozoic platform-basin margin: The Gargano fault system, Adria, Italy. Geosphere 3 (1), 1-15.

Borre, K., Cacon, S., Cello, G., Kontny, B., Kostak, B., Likke Andersen, H., Moratti, G., Piccardi, L., Stemberk, J., Tondi, E., Vilimek, V., 2003. The COST project in Italy: analysis and monitoring of seismogenic faults in the Gargano and Norcia areas (central southern Apennines, Italy). J. Geodyn. 36, 3-18.

Boschi, E., Guidoboni, E., Ferrari, G., Mariotti, D., Valensise, G., Gasperini, P., eds., 2000. Catalogue of strong italian earthquakes from 461 B.C. to 1997, Ann. Geophys. 43, with CD-Rom, 259 p. On-line version 3.1 on: http://storing.ingv.it/cft/

Bosellini, A., Neri, C., Luciani, V., 1993. Guida ai carbonati cretaceo-eocenici di scarpata e bacino del Gargano (Italia meridionale). Annali dell'Università di Ferrara (Nuova serie), Sezione: Scienze della Terra; vol. 4, Supplemento, 77 p.

Butler, R.W.H., Mazzoli, S., Corrado, S., De Donatis, M., Scrocca, D., Di Bucci, D., Gambini, R., Naso, G., Nicolai, C., Shiner, P. and Zucconi, V., 2004. Applying thick-skinned tectonic models to the Apennine thrust belt of Italy - Limitations and implications. In: Thrust tectonics and hydrocarbon systems (K.R. McClay, ed.). Amer. Ass. Petrol. Geol. Memoir 82, 647-667.

Calcagnile, G., Panza, G.F., 1981. The main characteristics of the lithosphere-asthenosphere system in Italy and surrounding regions. Pure and Applied Geophysics 119, 865-879.

Casnedi, R., Moruzzi, G., 1978. Geologia del campo gassifero di Chieuti (Foggia). Boll. Soc. Geol. It. 97 (3), 189-196.

Castello, B., Selvaggi, G., Chiarabba, C., Amato, A., 2006. CSI Catalogo della sismicità italiana 1981-2002, versione 1.1. INGV-CNT, Roma http://www.ingv.it/CSI/

Catalano, R., Doglioni, C., Merlini, S., 2001. On the Mesozoic Ionian Basin. Geophys. J. Int. 144, 49-64.

Cattaneo, A., Correggiari, A., Langone, L., Trincardi, F. 2003. The late-Holocene Gargano subaqueous delta, Adriatic shelf: sediment pathways and supply fluctuations. Marine Geology 193, 61-91.

Channell, J.E.T., D'Argenio, B., Horwath, F., 1979. Adria, the African promontory, in Mesozoic Mediterranean paleogeography. Earth Sc. Rev. 15, 213-292.

Chiappini, M., Meloni, A., Boschi, E., Faggioni, O., Beverini, N., Carmisciano, C., Marson, I., 2000. Shaded relief magnetic anomaly map of Italy and surrounding marine areas. Ann. Geophys. 43 (5), 983-989.
Chiarabba C., Jovane, L., Di Stefano, R., 2005. A new view of Italian seismicity using 20 years of instrumental recordings. Tectonophysics 395, 251– 268.
Chilovi, C., De Feyter, A.J., Pompucci, A., 2000. Wrench zone reactivation in the Adriatic Block: the example of the Mattinata Fault System (SE Italy). Boll. Soc. Geol. It. 119 (1), 3-8.
Christie-Blick, N., Biddle, E, K.T., 1985. Deformation and Basin formation along strike-slip faults. In: Strike-slip deformation, basin formation, and sedimentation (Biddle, E, K.T., Christie-Blick, N., eds.). Soc. Ec. Pal. Min. Special Publication 37, 1-34.
Ciaranfi, N., Pieri, P., Ricchetti, G., 1988. Note alla carta geologica delle Murge e del Salento (Puglia centro-meridionale). Mem. Soc. Geol. It. 41, 449-460.
Cinque, A., Patacca, E., Scandone, P., Tozzi, M., 1993. Quaternary kinematic evolution of the southern Apennines. Relationship between surface geological features and deep lithospheric structures. Annali di Geofisica 36, 249-260.
Colantoni, P., Tramontana, M., Tedeschi, R., 1990. Contributo alla conoscenza dell'avampaese apulo: struttura del Golfo di Manfredonia (Adriatico meridionale). Giornale di Geologia, serie 3a, 52 (1-2), 19-32.
Correggiari, A., Trincardi, F., Langone, L., Roveri, M., 2001. Styles of failure in late Holocene highstand prodelta wedges on the Adriatic shelf. J. Sed. Res. 71 (2), 218-236.
D'Agostino, N., Jackson, J.A., Dramis, F., Funiciello, R., 2001. Interactions between mantle upwelling, drainage evolution and active normal faulting: an example from the central Apennines (Italy). Geophys. J. Int. 147, 475-497.
de Alteriis, G., Aiello, G., 1993. Stratigraphy and tectonics offshore of Puglia (Italy, Southern Adriatic Sea). Marine Geology 113, 233-253.
de Alteriis, G., 1995. Different foreland basins in Italy: examples from the central and southern Adriatic Sea. Tectonophysics 252, 349-373.
De' Dominicis, A., Mazzoldi, G., 1987. Interpretazione geologico-strutturale del margine orientale della Piattaforma apula. Mem. Soc. Geol. It. 38, 163-176.
Di Bucci, D., Mazzoli, S., 2003. The October-November 2002 Molise seismic sequence (southern Italy): an expression of Adria intraplate deformation. J. Geol. Soc. London 160, 503-506.
Di Bucci, D., Ravaglia, A., Seno, S., Toscani, G., Fracassi, U., Valensise, G., 2006. Seismotectonics of the Southern Apennines and Adriatic foreland: insights on active regional E-W shear zones from analogue modeling. Tectonics 25, TC4015, doi:10.1029/2005TC001898.
DISS Working Group, 2006. Database of Individual Seismogenic Sources (DISS), Version 3.0.2: A compilation of potential sources for earthquakes larger than M 5.5 in Italy and surrounding areas. http://www.ingv.it/DISS/, © INGV 2005, 2006 - Istituto Nazionale di Geofisica e Vulcanologia - All rights reserved.
Doglioni, C., Mongelli, F., Pieri, P., 1994. The Puglia uplift (SE-Italy): an anomaly in the foreland of the Apenninic subduction due to buckling of a thick continental lithosphere. Tectonics 13, 1309-1321.
Favali, P., Funiciello, R., Mattietti, G., Mele, G., Salvini, F., 1993. An active margin across the Adriatic Sea central Mediterranean Sea). Tectonophysics 219, 109-117.
Ferranti, L., Oldow, J., 2005. Latest Miocene to Quaternary horizontal and vertical displacement rates during simultaneous contraction and extension in the Southern Apennines orogen, Italy. Terra Nova 17, 209-214.
Finetti, I., 1982. Structure, stratigraphy and evolution of the Central Mediterranean. Boll. Geofis. Teor. Appl. 24, 247-312.
Finetti, I., 1984. Struttura ed evoluzione della microplacca Adriatica (Structure and evolution of the Adriatic microplate). Boll. Ocean. Teor. Appl. II (2), 115-123.
Funiciello, R., Montone, P., Salvini, F., Tozzi, M., 1988. Caratteri strutturali del Promontorio del Gargano. Mem. Soc. Geol. It. 41, 1235-1243.
Galadini, F., 1999. Pleistocene changes in the central Apennine fault kinematics: A key to decipher active tectonics in central Italy. Tectonics 18, 877-894.
Galadini, F., Meletti, C., Vittori, E., 2001. Major active faults in Italy: available surficial data. Netherlands J. Geosci. 80, 273-296.
Giuliani, R., Anzidei, M., Bonci, L., Calcaterra, S., D'Agostino, N., Mattone, M., Pietrantonio, G., Riguzzi, F., Selvaggi, G., 2007. Co-seismic displacements associated to the Molise (Southern Italy) earthquake

sequence of October-November 2002 inferred from GPS measurements. Tectonophysics 432, 21-35.
Gruppo di Lavoro CPTI, 2004. Catalogo Parametrico dei Terremoti Italiani, versione 2004 (CPTI04). INGV, Bologna, http://emidius.mi.ingv.it/CPTI/
Helland-Hansen, W., Martinsen, O.J., 1996. Shoreline trajectories and sequences: description of various depositional-dip scenarios. J. Sed. Res. 66B, 670-688.
Mariotti, G., Doglioni, C., 2000. The dip of the foreland monocline in the Alps and Apennines. Earth Planet. Sc. Lett. 181, 191-202.
MEDNET, 2006. MEDiterranean Very Broadband Seismographic NETwork, INGV, http://mednet.rm.ingv.it/events/Welcome.html.
Montone, P., Mariucci, M.T., Pondrelli, S., Amato, A., 2004. An improved stress map for Italy and surrounding regions (central Mediterranean). J. Geophys. Res. 109, B10410, 1-22, doi: 10.1029/1003JB002703.
Morelli, D., 2002. Evoluzione tettonico-stratigrafica del Margine Adriatico compreso tra il Promontorio garganico e Brindisi. Mem. Soc. Geol. It. 57, 343-353.
Mostardini, F., Merlini, S., 1986. Appennino centro-meridionale. Sezioni Geologiche e Proposta di Modello Strutturale. Mem. Soc. Geol. It. 35, 177-202.
Ortolani, F., Pagliuca, S. 1987. Tettonica transpressiva nel Gargano e rapporti con le Catene Appenninica e Dinarica. Mem. Soc. Geol. It. 38, 205-224.
Patacca, E., Scandone, P., 1989. Post-Tortonian mountain building in the Apennines. The role of the passive sinking of a relic lithospheric slab. In: The Lithosphere in Italy (Boriani, A.M., Bonafede, M., Piccardo, G.B., Vai, G.B., eds.). Atti dei Convegni Lincei 80, 157-176.
Patacca, E., Scandone, P., 2004a. The 1627 Gargano earthquake (Southern Italy): Identification and characterization of the causative fault. J. Seismol. 8 (2), 259-273.
Patacca, E., Scandone, P., 2004b. The Plio-Pleistocene thrust belt – foredeep system in the Southern Apennines and Sicily (Italy). In: Geology of Italy (Crescenti, U., D'Offizi, S., Merlini, S., Lacchi, L., eds.). Soc. Geol. It., Roma, 93-129.
Piccardi, L., 1998. Cinematica attuale, comportamento sismico e sismologia storica della faglia di Monte S. Angelo (Gargano, Italia): la possibile rottura superficiale del "leggendario" terremoto del 493 d.C. Geogr. Fis. Dinam. Quat. 21, 155-166.
Piccardi, L., 2005. Paleoseismic evidence of legendary earthquakes: The apparition of Archangel Michael at Monte Sant'Angelo (Italy). Tectonophysics 408, 113–128.
Ricchetti, G., Ciaranfi, N., Luperto Sinni, E., Mongelli, F., Pieri, P., 1988. Geodinamica ed evoluzione sedimentaria e tettonica dell'avampaese apulo. Mem. Soc. Geol. It. 41, 57-82.
Ricci Lucchi, F., 1986. The Oligocene to Recent foreland basins of the Northern Apennines. In: Foreland basins (Allen, P.A., Homewood, P., eds.). Int. Ass. Sed. Special Publication 8, 105-139.
Ridente, D., Foglini, F., Minisini, D., Trincardi, F., Verdicchio, G., 2007. Shelf-edge erosion, sediment failure and the Middle Pleistocene inception of Bari Canyon on the South-Western Adriatic Margin (Central Mediterranean). Marine Geology 239, doi: 10.1016/j.margeo.2007.01.014.
Ridente, D., Trincardi, F., 2002a. Eustatic and tectonic control on deposition and lateral variability of Quaternary regressive sequences in the Adriatic basin (Italy). Marine Geology 184 (3-4), 273-293.
Ridente, D., Trincardi, F., 2002b. Late Pleistocene depositional cycles and syn-sedimentary tectonics on the Adriatic shelf. Mem. Soc. Geol. Ital., Vol. Spec. 57, 517-526.
Ridente, D., Trincardi, F., 2005. Pleistocene ''muddy'' forced-regression deposits on the Adriatic shelf: a comparison with prodelta deposits of the late Holocene highstand mud wedge. Marine Geology 222-223, 213-233.
Ridente, D., Trincardi, F., 2006. Active foreland deformation evidenced by shallow folds and faults affecting late Quaternary shelf-slope deposits (Adriatic Sea, Italy). Basin Research 18 (2), 171-188. doi: 10.1111/j.1365-2117.2006.00289.x
Rodriguez, J.A., Audemard, F.A., 2003. Sobrestimaciones y limitaciones en los estudios de sismicidad histórica con base en casos venezolanos. Revista Geográfica Venezolana 44 (1), 47-75.
Royden, L.E., Patacca, E., Scandone, P., 1987. Segmentation and configuration of subducted lithosphere in Italy: an important control on thrust-belt and foredeep-basin evolution. Geology 15, 714-717.
Salvini, F., Billi, A., Wise, D.U., 1999. Strike-slip fault-propagation cleavage in carbonate rocks: the Mattinata Fault Zone, Southern Apennines, Italy. J. Struct. Geol. 21, 1731-1749.
Stucchi, M., Camassi, R., Rovida, Locati, M., Ercolani, E., Meletti, C., Migliavacca,P., Bernardini, F., Azzaro, R., 2007. DBMI04, il database delle osservazioni macrosismiche dei terremoti italiani

utilizzate per la compilazione del catalogo parametrico CPTI04. http://emidius.mi.ingv.it/DBMI04/ Quaderni di Geofisica, INGV, accepted.

Tiberti, M.M., Orlando, L., Di Bucci, D., Bernabini, M., Parotto, M., 2005. Regional gravity anomaly map and crustal model of the Central-Southern Apennines (Italy). Journal of Geodynamics 40, 73-91.

Tondi, E., Piccardi, L., Cacon, S., Kontny, B., Cello, G., 2005. Structural and time constraints for dextral shear along the seismogenic Mattinata fault (Gargano, southern Italy). J. Geodyn. 40, 134-152.

Tramontana, M., Morelli, D., Colantoni, P., 1995. Tettonica plio-quaternaria del sistema sud-garganico (settore orientale) nel quadro evolutivo dell'Adriatico centro-meridionale. Studi Geol. Camerti, Volume Speciale 1995/2, 467-473.

Trincardi, F., Asioli, A., Cattaneo, A., Correggiari, A., Langone, L., 1996. Stratigraphy of the late-Quaternary deposits in the Central Adriatic basin and the record of short-term climatic events. In: Palaeoenvironmental analysis of Italian crater lake and Adriatic sediments (Guilizzoni, P., Oldfield, F.L. eds.). Mem. Istit. It. Idrob., 55, 39-64.

Trincardi, F., Correggiari, A., 2000. Quaternary forced regression deposits in the Adriatic basin and the record of composite sea-level cycles. In: Depositional Response to Forced Regression (Hunt, D., Gawthorpe, R., eds.). Geol. Soc. Special Publication 172, 245-269.

Valensise, G., Pantosti, D., eds., 2001. Database of Potential Sources for Earthquakes Larger than M 5.5 in Italy. Ann. Geophys. 44 (1), with CD-ROM.

Valensise, G., Pantosti, D., Basili, R., 2004. Seismology and Tectonic Setting of the Molise Earthquake Sequence of October 31-November 1, 2002. Earthq. Spectra 20 (1), 23-37.

Vallée, M., Di Luccio, F., 2005. Source analysis of the 2002 Molise, southern Italy, twin earthquakes (10/31 and 11/01). Geophys. Res. Lett. 32, L12309, 1-4, doi:10.1029/2005GL022687

Vannucci, G., Gasperini, G., 2004. The new release of the Database of Earthquake Mechanisms of the Mediterranean Area (EMMA version 2). Ann. Geophys. 47 (1), with CD-Rom.

Wells, D.L., Coppersmith, K.J., 1994. New empirical relationships among magnitude, rupture length, rupture width, rupture area, and surface displacement. Bull. Seismol. Soc. Am. 84 (4), 974-1002.

Winter, T., Tapponnier, P., 1991. Extension majeure post-Jurassique et ante-Miocene dans le centre de l'Italie: données microtectoniques. Bull. Soc. Géol., France 162 (6), 1095-1108.

Wortmann, U.G., Weissert, H., Funk, H., Hauck, J., 2001. Alpine plate kinematics revisited: The Adria problem. Tectonics 20, 134-147.

Figure captions

Fig. 1: a) Geological sketch map of Southern Italy (Calabrian arc excluded), showing the Mattinata-Gondola Shear Zone (MGSZ). b) Historical and instrumental earthquakes of the Central and Southern Apennines (M > 4.0; Gruppo di lavoro CPTI, 2004; Vannucci and Gasperini, 2004). The size of the square symbols is proportional to an equivalent magnitude derived from intensity data.

Fig. 2: High-resolution (Chirp-Sonar and Sparker) seismic database used to define the stratigraphy of Late Quaternary deposits and the pattern of active deformation in the southern Adriatic Foreland. The box bounds the shelf area where deformation has been mapped in detail (Fig. 5). Note the complex morphology of the shelf margin (affected by large-scale erosion) and slope, where the relief along the NW-SE strike of the Gondola Fault Zone culminates in the Dauno Seamount (compare with Fig. 3).

Fig. 3: Previous studies on the structural setting of the Gondola Fault Zone and nearby areas, based on high-penetration/low-resolution seismic data, all simplified and redrawn from: a) De' Dominicis and Mazzoldi (1987); b) Colantoni et al. (1990); c) de Alteriis (1995); d) Morelli (2002). Symbols for wells and locations are given in a). Notice the variable definitions of the Gondola Fault Zone.

Fig. 4: Seismic profile SE06-62, summarising all key stratigraphic and structural features of the study area (notice the vertical exaggeration of Chirp-Sonar seismic profiles). Two gentle anticlines and an interposed syncline affect deposits overlying the inherited Gondola Fault Zone, located deep below the section. Both anticlines are slightly asymmetric, with a steeper northern limb. The northern anticline is affected by high-angle faults and secondary undulations. The southern one shows fluid-escape features and a minor undulation, likely indicating incipient fault propagation (dashed arrows). The folds are sealed by ES1 (~20 ka BP) and are characterised by syn-tectonic units within sequence 2 (dated between 230-250 and 130-150 ka BP) throughout the entire area. Faults in the section exhibit a vertical component of motion. Notice that both the main fault and its antithetic one displace the 5.5 ka maximum flooding surface (mfs) and the seafloor, where a small graben is detectable.

Fig. 5: Structural map of the investigated area. 1) faults affecting the Holocene and Middle-Upper Pleistocene deposits; 2) faults affecting only the Middle-Upper Pleistocene deposits; 3) crest lines of the major anticlines; 4) crest lines of the minor anticlines and undulations; 5) flex lines of the fold limbs; 6) synclines; 7) fluid-escape features; 8) seafloor depth contours (interval 5 m). Thin straight

lines show the trace of seismic profiles in Figs. 4, 6, 7 and 8. Two major anticlines (northern and southern) and three main fault branches (western, central and eastern) can be identified. The fault branches show variable extent and may appear sealed by the ES1 surface or displace the Holocene deposits and the sea floor. They show a vertical component of motion, with the northern limb downthrown. In the easternmost part of the study area, close to the shelf-slope transition and in contrast with the pattern observed all along the rest of the Gondola Fault Zone, the southern limb is downthrown.

Fig. 6: Examples of Chirp Sonar seismic profiles crossing the three fault branches. A) The northern fold is affected by a fault abruptly displacing Middle-Upper Pleistocene deposits and truncated by ES1. Notice the erosion and incision of deposits of sequence 1 on the limbs of the anticline, and the thickness reduction of sequence 2. A minor undulation is evident on the northern limb of the anticline. B) The fold along the central branch is markedly asymmetric, limited to the north by a fault affecting uppermost Pleistocene and Holocene deposits, up to the seafloor. C) In the eastern part of the study area, the southern fold appears more asymmetric than the northern one. Notice that the fault is located near the axis of the northern fold and offsets the reflectors up to the seafloor. See Figs. 2 and 5 for location.

Fig. 7: Evidence of a secondary fold on the downthrown (northern) limb of the western branch fault, interpreted as the expression of an unresolved strike-slip component. Also notice the variable offset of reflectors along the fault plane.

Fig. 8: Interpretation of Sparker profile SE-64. Deformation affects depositional units older than sequence 4, commonly not imaged on Chirp data, and is accompanied by growth strata at the base of sequence 4. Syn-tectonic deposits are also evident at the base of sequence 3, thus indicating fold growth at variable rates also before the time span commonly investigated using Chirp data. The section also shows syn-tectonic features within sequence 2, that may be related to shelf margin incision and large scale erosion. Note the presence of a high-angle fault coinciding with the axis of the anticline, characterised by southern side downthrown and by the progressive decrease of the offset of reflectors from older to younger deposits.

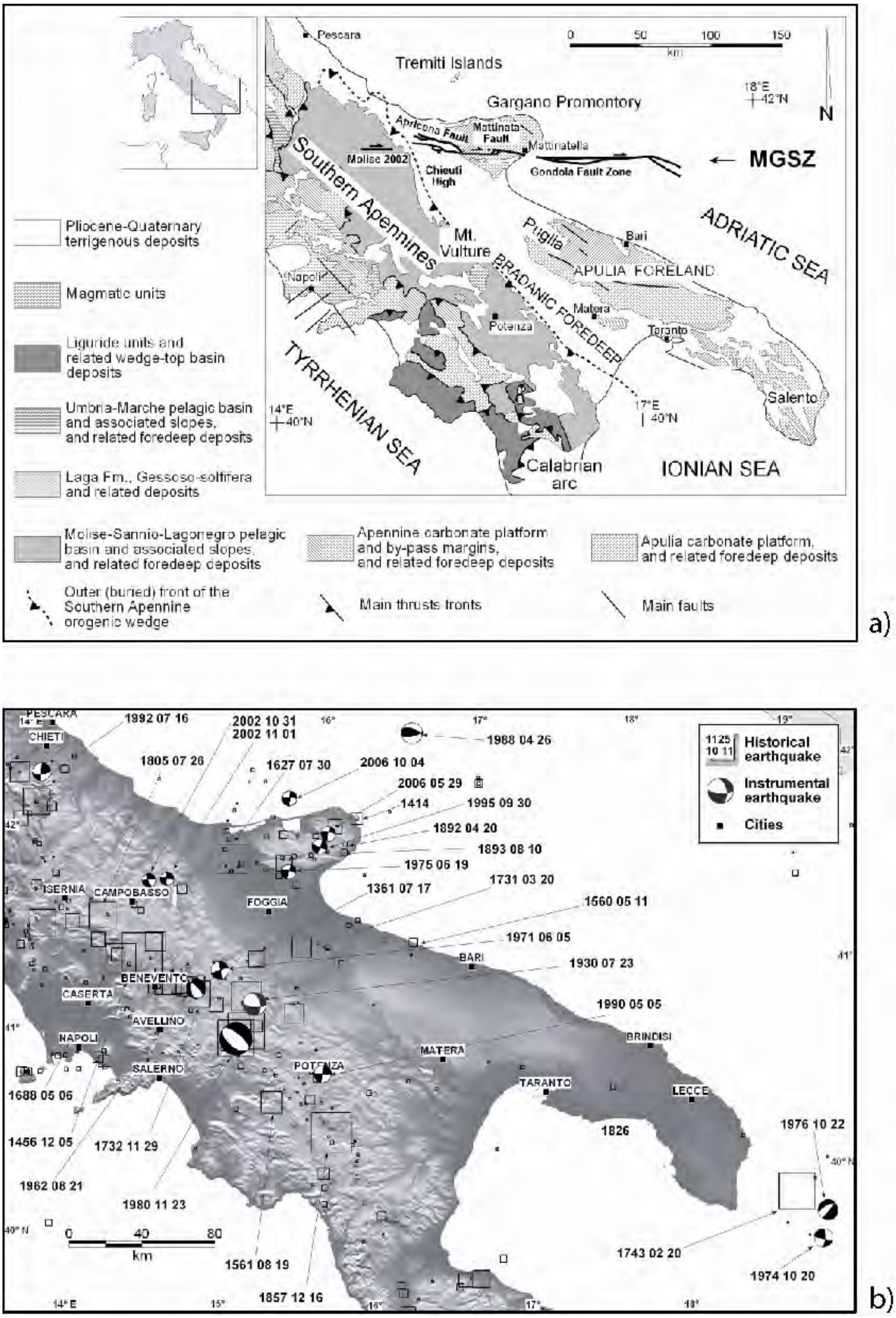
Pescara
Tremiti Islands
Gargano Promontory
Apricena Fault
Mattinata Fault
Mattinatella
Molise 2002
Chieuti High
Gondola Fault Zone
MGSZ
N
Southern Apennines
Mt. Vulture
Puglia
Bari
ADRIATIC SEA
APULIA FORELAND
BRADANIC FOREDEEP
Napoli
Potenza
Matera
Taranto
TYRRHENIAN SEA
Calabrian arc
IONIAN SEA
Salento
Pliocene-Quaternary terrigenous deposits
Magmatic units
Liguride units and related wedge-top basin deposits
Umbria-Marche pelagic basin and associated slopes, and related foredeep deposits
Laga Fm., Gessoso-solfifera and related deposits
Molise-Sannio-Lagonegro pelagic basin and associated slopes, and related foredeep deposits
Apennine carbonate platform and by-pass margins, and related foredeep deposits
Apulia carbonate platform, and related foredeep deposits
Outer (buried) front of the Southern Apennine orogenic wedge
Main thrusts fronts
Main faults
a)
Historical earthquake
Instrumental earthquake
Cities
PESCARA
CHIETI
ISERNIA
CAMPOBASSO
FOGGIA
BENEVENTO
CASERTA
AVELLINO
NAPOLI
SALERNO
POTENZA
MATERA
BARI
BRINDISI
TARANTO
LECCE
1992 07 16
2002 10 31
2002 11 01
1988 04 26
1805 07 26
1627 07 30
2006 10 04
2006 05 29
1414
1995 09 30
1892 04 20
1893 08 10
1975 06 19
1731 03 20
1361 07 17
1560 05 11
1971 06 05
1930 07 23
1990 05 05
1688 06 06
1456 12 05
1732 11 29
1962 08 21
1980 11 23
1826
1976 10 22
1743 02 20
1974 10 20
1561 08 19
1857 12 16
km
b)

Fig. 1

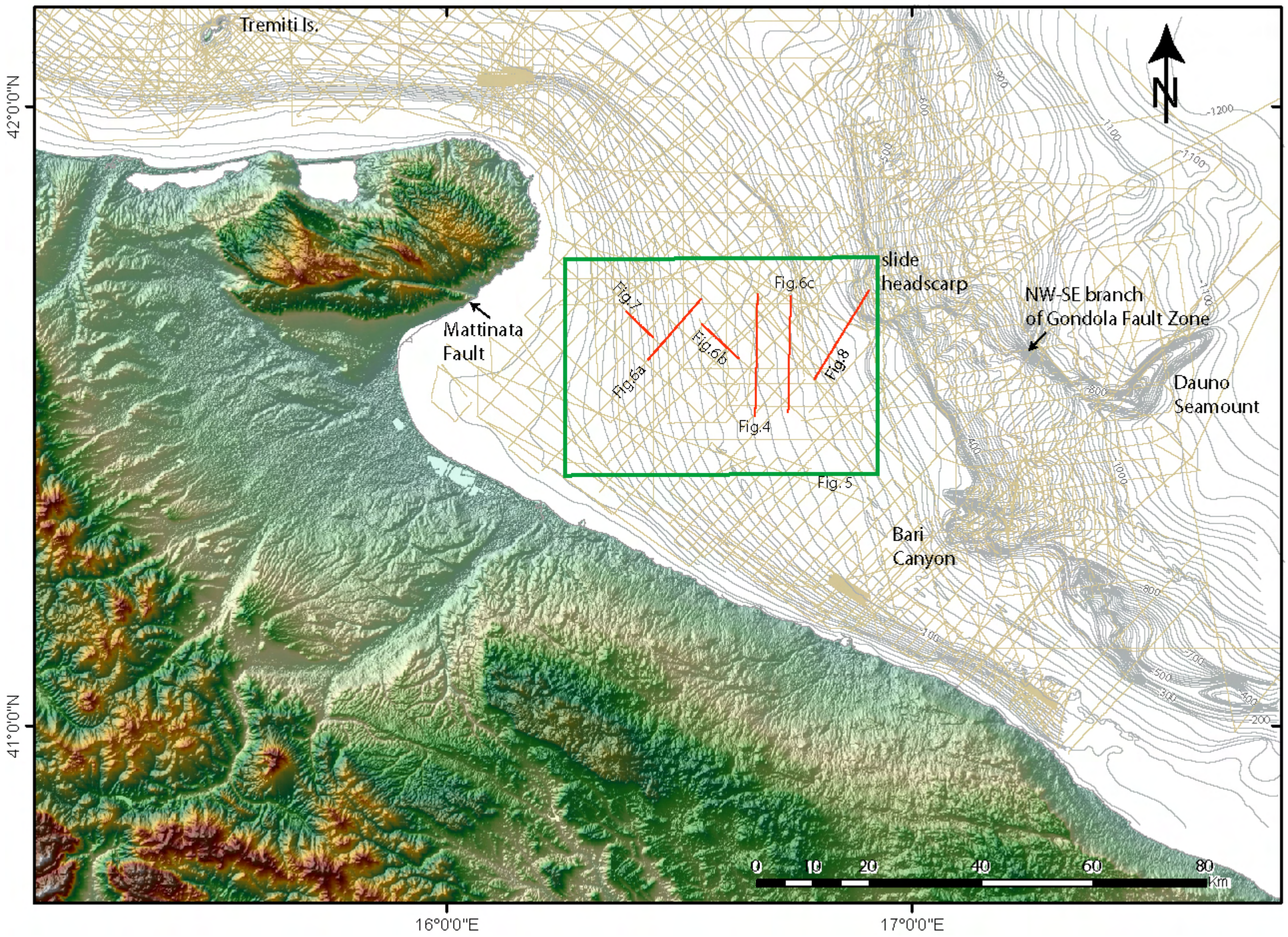
Tremiti Is.
42°0'0"N
41°0'0"N
16°0'0"E
17°0'0"E
N
Mattinata
Fault
slide
headscarp
NW-SE branch
of Gondola Fault Zone
Dauno
Seamount
Bari
Canyon
Fig.7
Fig.6a
Fig.6b
Fig.6c
Fig.4
Fig.8
Fig. 5
0 10 20 40 60 80
Km

Fig. 2

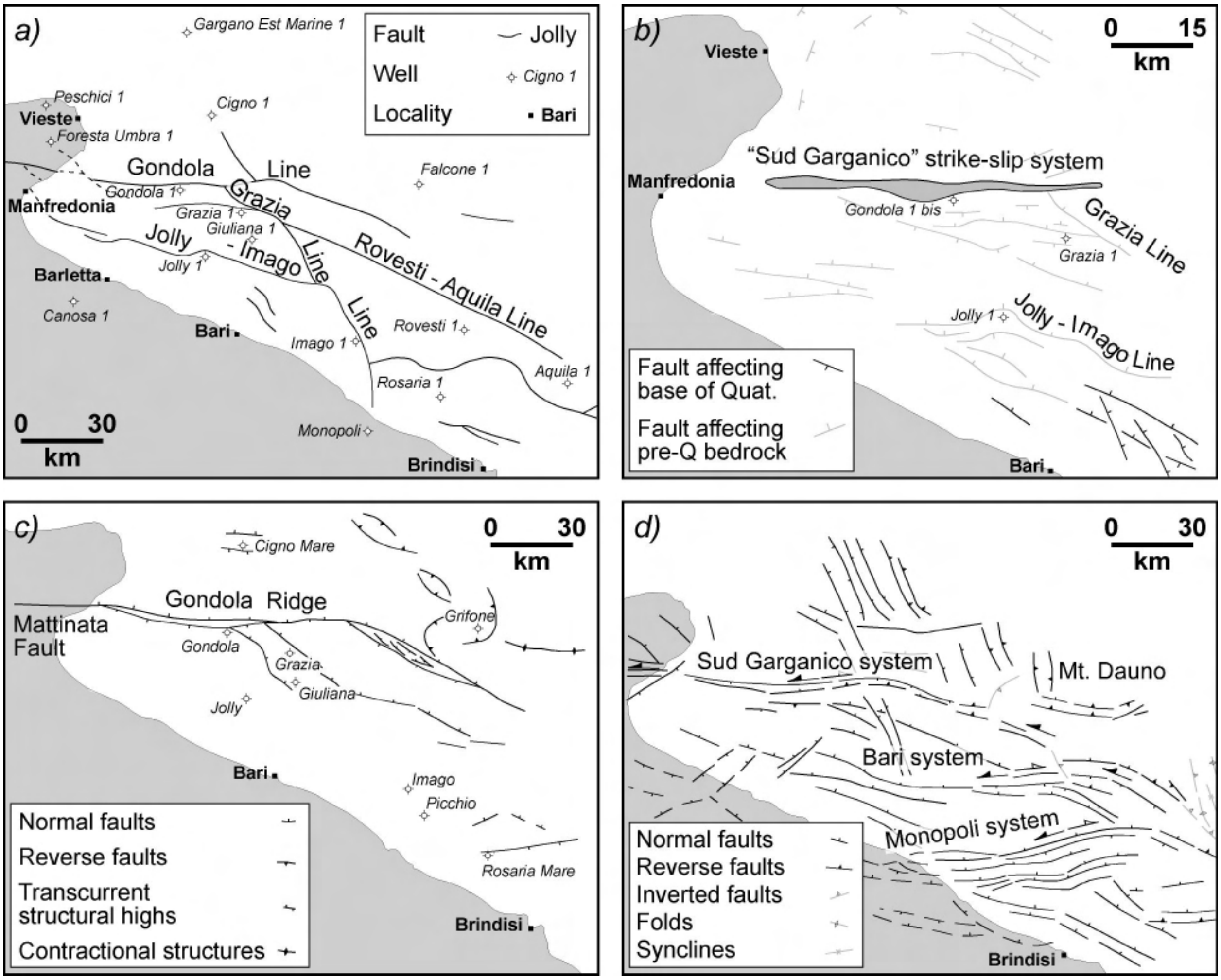
a)
Gargano Est Marine 1
Fault
Jolly
Well
Cigno 1
Locality
Bari
Peschici 1
Vieste
Foresta Umbra 1
Cigno 1
Gondola
Line
Falcone 1
Gondola 1
Manfredonia
Grazia
Grazia 1
Giuliana 1
Jolly
- Imago
Line
Rovesti - Aquila Line
Jolly 1
Barletta
Canosa 1
Bari
Imago 1
Rovesti 1
Line
Aquila 1
Rosaria 1
Monopoli
Brindisi
0 30
km
b)
Vieste
0 15
km
"Sud Garganico" strike-slip system
Manfredonia
Gondola 1 bis
Grazia Line
Grazia 1
Jolly 1
Jolly - Imago Line
Fault affecting base of Quat.
Fault affecting pre-Q bedrock
Bari
c)
Cigno Mare
0 30
km
Gondola Ridge
Mattinata Fault
Grifone
Gondola
Grazia
Giuliana
Jolly
Bari
Imago
Picchio
Rosaria Mare
Brindisi
Normal faults
Reverse faults
Transcurrent structural highs
Contractional structures
d)
0 30
km
Sud Garganico system
Mt. Dauno
Bari system
Monopoli system
Normal faults
Reverse faults
Inverted faults
Folds
Synclines
Brindisi

Fig. 3

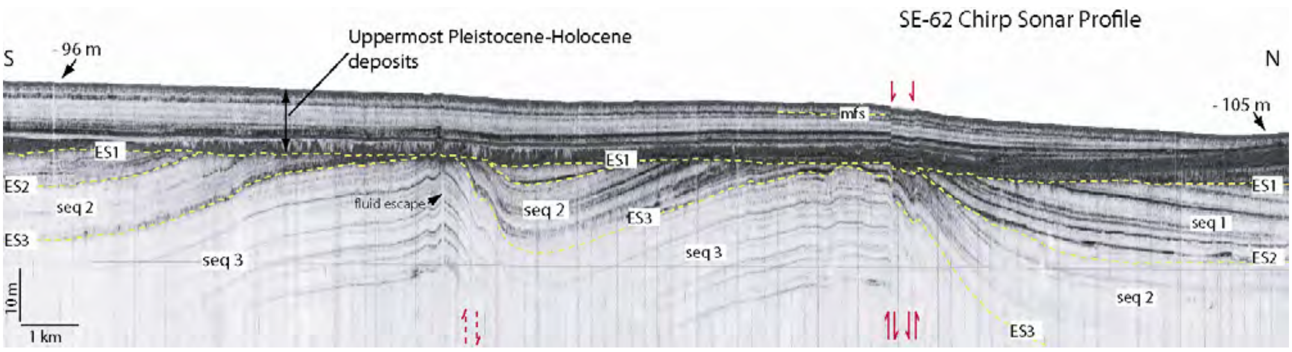
SE-62 Chirp Sonar Profile
Uppermost Pleistocene-Holocene deposits
S
- 96 m
N
- 105 m
mfs
ES1
ES2
ES3
seq 1
seq 2
seq 3
fluid escape
10 m
1 km

Fig. 4

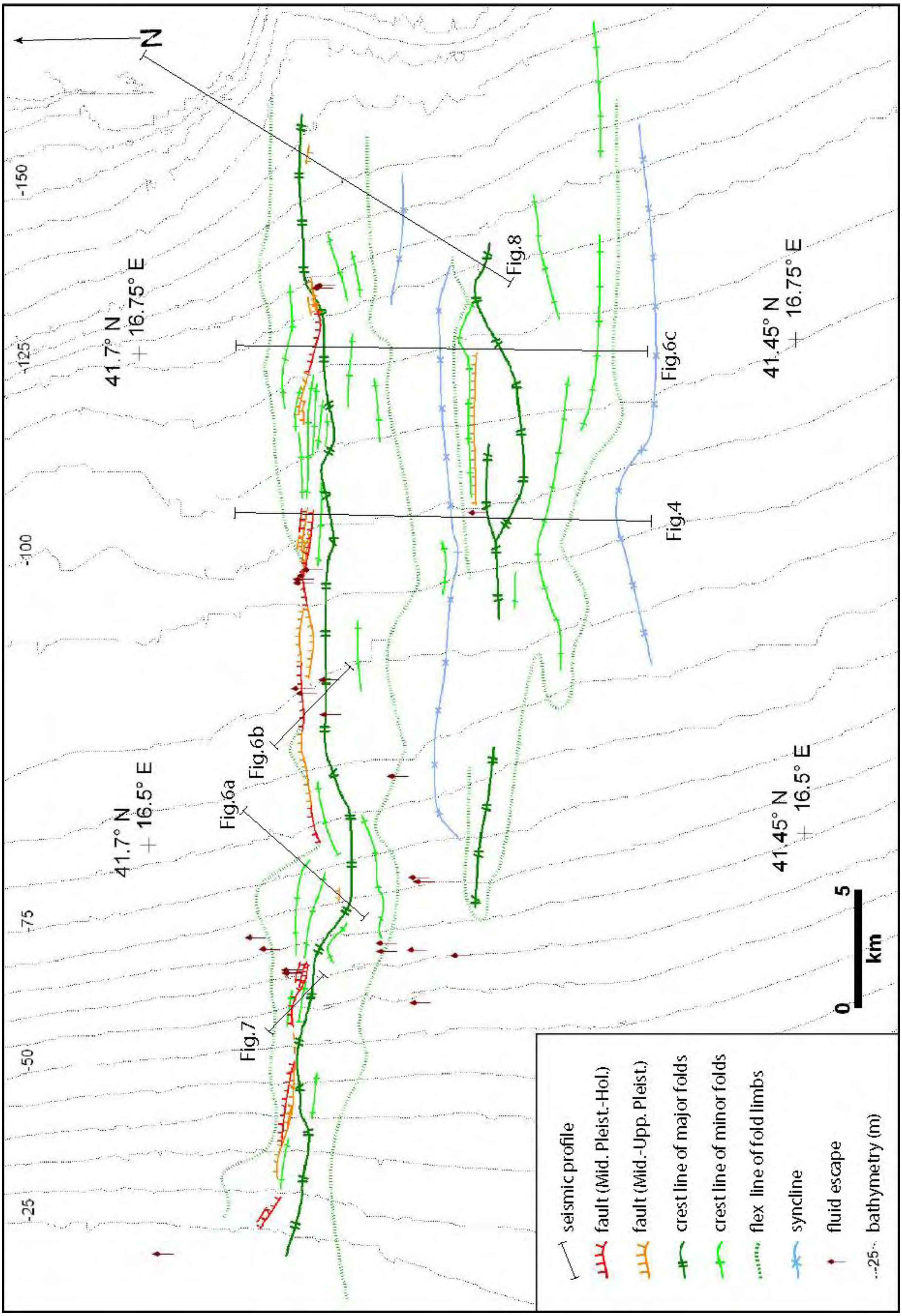
N
-150
-125
-100
-75
-50
-25
41.7° N
16.75° E
41.7° N
16.5° E
41.45° N
16.75° E
41.45° N
16.5° E
Fig.8
Fig.6c
Fig.4
Fig.6b
Fig.6a
Fig.7
0
5
km
seismic profile
fault (Mid. Pleist.-Hol.)
fault (Mid.-Upp. Pleist.)
crest line of major folds
crest line of minor folds
flex line of fold limbs
syncline
fluid escape
-25- bathymetry (m)

Fig. 5

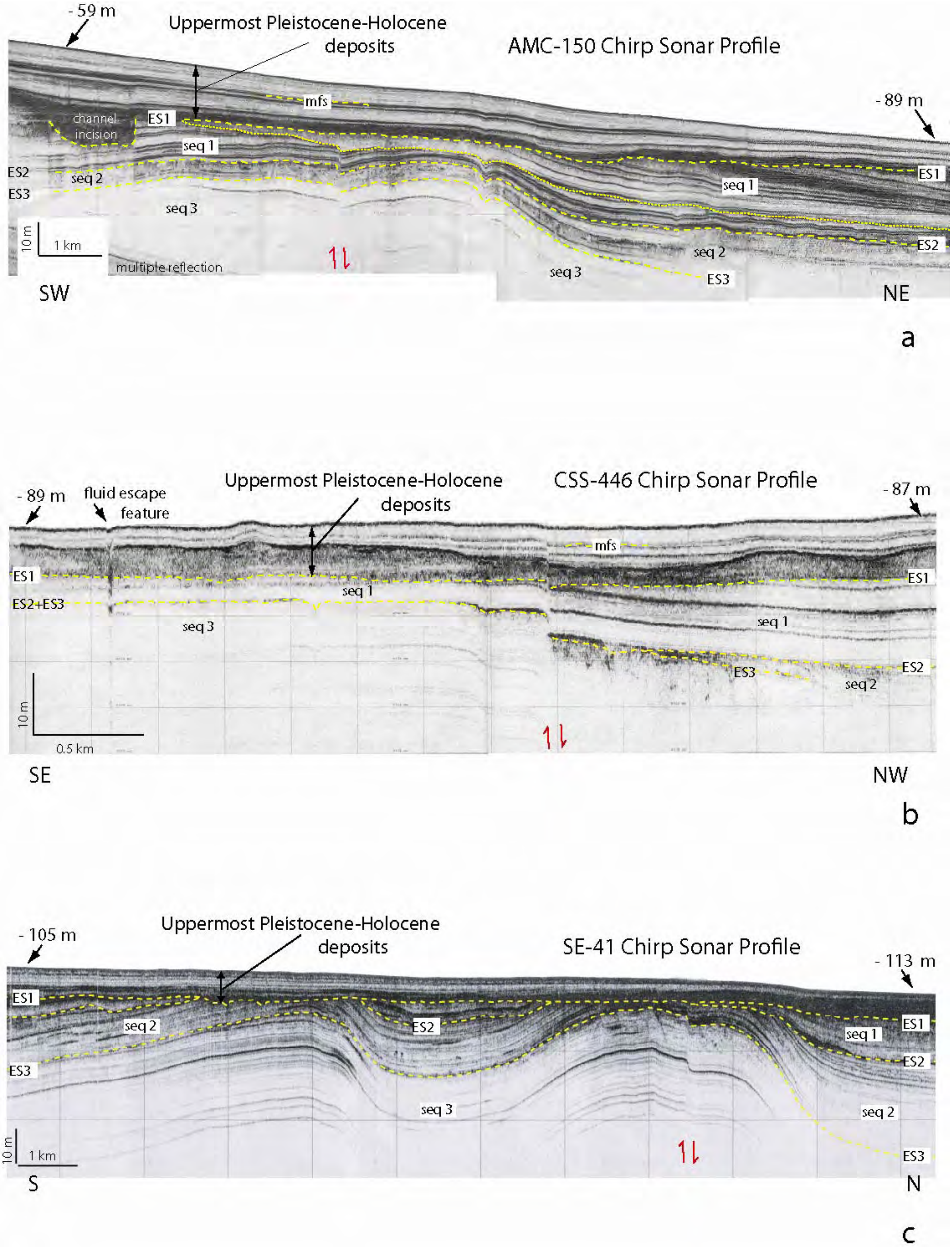
- 59 m
Uppermost Pleistocene-Holocene deposits
AMC-150 Chirp Sonar Profile
mfs
- 89 m
channel incision
ES1
seq 1
ES2
ES3
seq 2
seq 3
10 m
1 km
multiple reflection
SW
NE
a
- 89 m
fluid escape feature
Uppermost Pleistocene-Holocene deposits
CSS-446 Chirp Sonar Profile
- 87 m
mfs
ES1
ES2+ES3
seq 1
seq 3
ES3
ES2
seq 2
10 m
0.5 km
SE
NW
b
- 105 m
Uppermost Pleistocene-Holocene deposits
SE-41 Chirp Sonar Profile
- 113 m
ES1
seq 2
ES2
ES3
seq 1
seq 3
10 m
1 km
S
N
c

Fig. 6

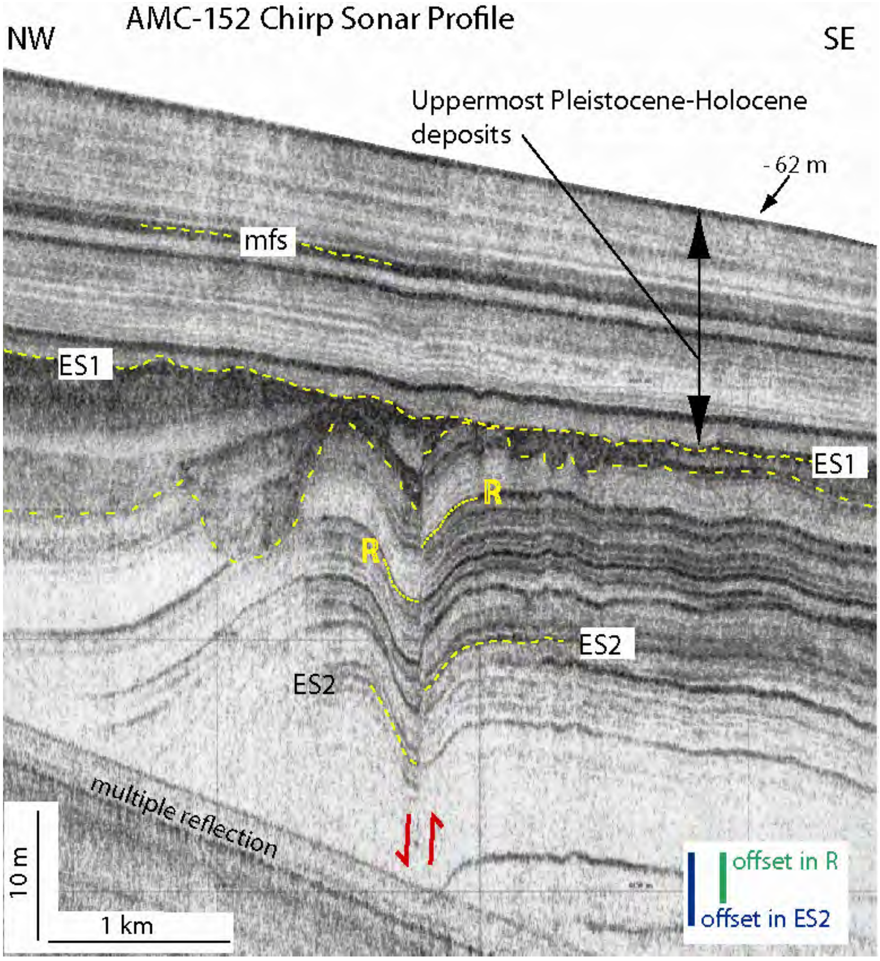
AMC-152 Chirp Sonar Profile
NW
SE
Uppermost Pleistocene-Holocene deposits
- 62 m
mfs
ES1
ES1
R
R
ES2
ES2
multiple reflection
10 m
1 km
offset in R
offset in ES2

Fig. 7

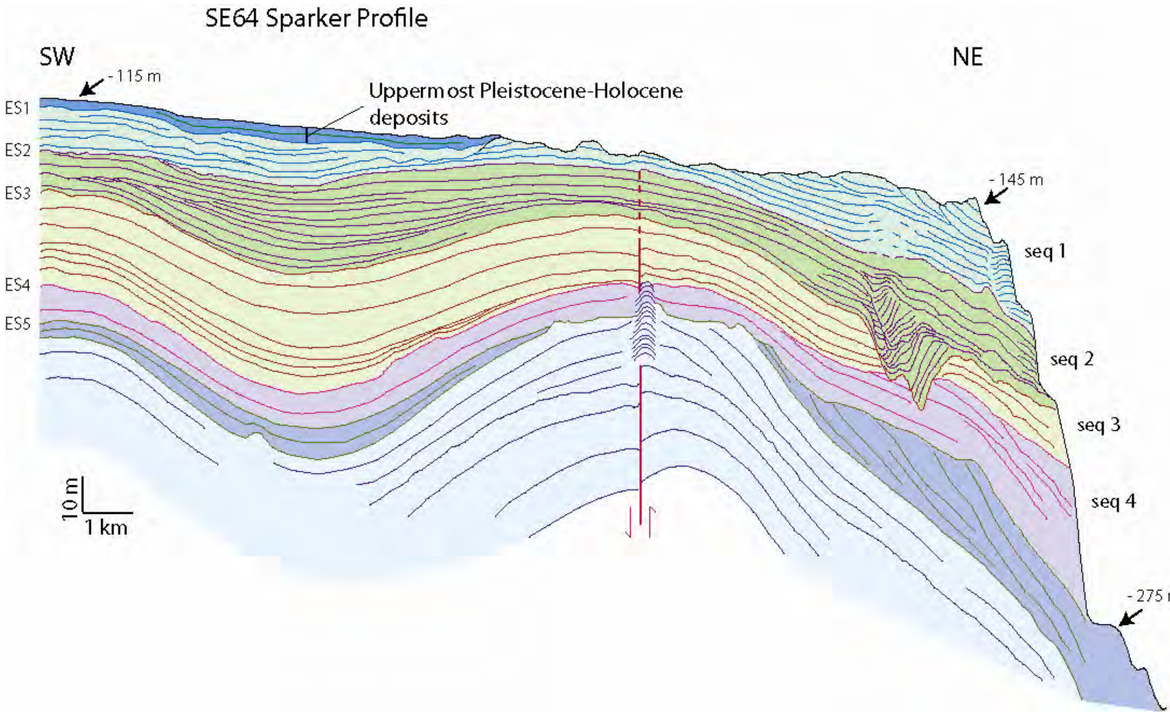
SE64 Sparker Profile
SW
NE
- 115 m
Uppermost Pleistocene-Holocene deposits
ES1
ES2
ES3
ES4
ES5
- 145 m
seq 1
seq 2
seq 3
seq 4
10 m
1 km
- 275 m

Fig. 8